

**Consume or Conserve: Microroughness of Titanium Implants
toward Fabrication of Dual Micro-Nanotopography**

Author

Gulati, Karan, Li, Tao, Ivanovski, Saso

Published

2018

Journal Title

ACS Biomaterials Science and Engineering

Version

Accepted Manuscript (AM)

DOI

[10.1021/acsbiomaterials.8b00829](https://doi.org/10.1021/acsbiomaterials.8b00829)

Rights statement

This document is the Accepted Manuscript version of a Published Work that appeared in final form in ACS Biomaterials Science and Engineering, © 2018 American Chemical Society after peer review and technical editing by the publisher. To access the final edited and published work see <https://doi.org/10.1021/acsbiomaterials.8b00829>

Downloaded from

<http://hdl.handle.net/10072/387566>

Griffith Research Online

<https://research-repository.griffith.edu.au>

Consume or Conserve: Micro-Roughness of Titanium Implants towards Fabrication of Dual Micro-Nano Topography

Karan Gulati ^{a,b,c} ✉, Tao Li ^{b,d}, and Sašo Ivanovski ^{a,b,c} ✉

^a The University of Queensland, School of Dentistry, Herston, QLD 4006, Australia

^b School of Dentistry and Oral Health, Griffith University, Gold Coast, QLD, Australia

^c Menzies Health Institute Queensland (MHIQ), Griffith University, Gold Coast, QLD, Australia

^d Department of Prosthodontics, School of Stomatology, Capital Medical University, Beijing, People's Republic of China

✉ Corresponding Author

Prof. Sašo Ivanovski (s.ivanovski@uq.edu.au) and Dr. Karan Gulati (k.gulati@uq.edu.au)

School of Dentistry, University of Queensland, 288 Herston Road, Herston QLD 4006, Australia

Keywords: titanium; implants; anodization; dual topography; nanopores; micro-rough

Abstract

Combining the micro-roughness of current titanium implants, which promotes accelerated bone integration, with nano-topography for enhanced bioactivity/drug-release may be an ideal solution to address therapeutic challenges inside the bone micro-environment. We hereby present a single-step electrochemical anodization using conditioned electrolyte to enable fabrication of aligned titania nanopores with preserved micro-scale features of the underlying titanium implant. Applicability towards the fabrication of mechanically robust and clinically translatable next-generation of orthopaedic/dental implants with dual-topography including 'gold-standard' micro-roughness and superimposed 'bioactive' nanotopography.

1
2
3 Electrochemical anodization (EA) of titanium resulting in self-ordering of titania
4 nanostructures (TNSs), such as nanotubes and nanopores, has gained considerable interest
5 with applications including bioactive and drug-eluting implants.¹⁻² It is accepted that
6 electrolyte preparation via repeated anodization (or ageing) results in improved ordering and
7 adherence of TNSs, especially in the case of organic electrolytes such as ethylene glycol.³⁻⁶ It
8 is worth noting that ageing optimizes the fluoride and water composition (especially in a
9 sealed electrochemical cell) of the electrolyte, which are crucial parameters for the formation
10 of TNSs.⁷ These parameters determine oxide growth/dissolution rates, O₂ evolution, barrier
11 layer thickness and the compressive stress at the titanium-oxide interface, which are inter-
12 dependent with each other and greatly influence the yield of the pores/tubes.⁷
13
14
15
16
17
18

19 Thus far, very few studies have focussed on understanding the influence of ageing on EA
20 of Ti, and hence there is a significant research gap and limited understanding of EA in this
21 domain. Most studies utilize an EA setup whereby the moisture uptake by the hygroscopic
22 electrolyte is a major consideration, as it is constantly increasing water content and hence
23 conductivity.³⁻⁶ Alternatively, more recently we have presented an extensive investigation
24 detailing the fabrication of TNS via electrolyte ageing in a sealed electrochemical setup.⁷
25 With this approach, water content continuously reduces and so does the conductivity.⁷ It was
26 established that ageing the electrolyte enables improved ordering and the formation of stable
27 nanostructures on the complex geometry of curved surfaces, representing a wider implant
28 market and hence easy translation. However, to advance our knowledge with respect to
29 electrolyte ageing and allow successful implant nano-engineering, it is crucial to understand
30 what happens at the metal-oxide interface, how the substrate topography influences the EA
31 and how the mechanical properties differ for TNS from fresh- and aged-electrolyte
32 anodizations.
33
34
35
36
37
38
39
40
41

42 In the case of biomedical applications of nano-engineered Ti, such as bone/dental
43 implants, the preservation of the underlying Ti implant features/roughness may be
44 particularly important for enabling initial interlocking/stability from the micro-features, and
45 then superimposing nanotubes/pores which may enable enhanced bioactivity or facilitate drug
46 release.⁸ These hybrid micro-nano topographies have been prepared in the past using more
47 complex lithography, laser-patterning or 3D printing, which have been combined with EA to
48 create nanotubes/pores.⁹⁻¹¹ Bypassing the conventional surface smoothing steps and
49 complex micro-patterning strategies, we hereby showcase a single-step EA on micro-
50 machined Ti implants which yields optimized micro-nano topographies. Titania nanopores
51
52
53
54
55
56
57
58
59
60

1
2
3 are fabricated instead of conventional nanotubes to augment the stability of the anodic film,
4 crucial for implant applications. The optimizations are performed using two electrolyte
5 systems: pre-utilized (aged) and un-used (fresh), while other parameters were controlled, to
6 also enable better understanding of the role of electrolyte conditioning in preserving the
7 underlying implant micro-scale features. Additionally, the mechanical testing of these
8 nanostructures obtained from varied electrolyte anodizations was also compared. The
9 fabrication of stable nanotopography with preserved micro-scale features of commercial
10 orthopaedic/dental implants could allow for multiple bioactive and therapeutic functionalities,
11 while enabling easy translation into current implant market.
12
13
14
15
16
17

18 Micro-machined Ti ('Micro-Ti') discs (6.24mm diameter, 2mm height, commercially
19 pure grade 4 Titanium) were supplied by AstraTech Dental (Sweden). Flat titanium foil
20 (99.5% purity, 0.2mm thick, 1 cm²) was purchased from Nilaco (Japan). Ethylene glycol and
21 ammonium fluoride (NH₄F) were purchased from Sigma-Aldrich (Sydney, Australia).
22 Surface topography of Ti implant substrates and the fabricated TNSs were investigated using
23 a scanning electron microscope (SEM, Zeiss Sigma FESEM). Titania nanopores (TNPs) were
24 fabricated via a single-step EA in a two-electrode electrochemical cell at 60-100V for various
25 times at room temperature using a DC power source (Keithley 2460) with the current
26 precisely monitored. The Micro-Ti discs with micro-groove features were used as an anode
27 and flat Ti foil served as the counter electrode. In this study, we performed anodizations in a
28 moisture-controlled system with an ethylene glycol electrolyte (with 0.3 wt% NH₄F and 1
29 vol% deionized water). Two different electrolytes were used for this study: fresh and aged.
30 "Fresh electrolyte" represents the newly prepared electrolyte without any previous use,
31 whereas "aged electrolyte" represents a previously used electrolyte, which was repetitively
32 anodized for 10h using dummy Ti, as previously described.⁷ To quantify the mechanical
33 properties of the fabricated nanoporous structures, elastic modulus and hardness
34 measurements were performed by nanoindentation testing, using a Berkovich 3-sided
35 pyramidal tip with a maximum force of 10,000 μN.
36
37
38
39
40
41
42
43
44
45
46

47 Figure 1 shows top-view SEM images of bare Micro-Ti, as well as anodized Micro-
48 Ti with either fresh or aged electrolyte. As received Micro-Ti (Figure 1a,b) shows
49 machined micro-scale lines and features, characteristic of the micro-roughness of
50 commercial implants. The average width of the 'sinusoidal' micro-features as
51 determined from SEM images is approximately 36 μm. Upon anodization, the micro-
52 features of the implant are better preserved with aged EA, with the 'crest-and-trough'
53
54
55
56
57
58
59
60

1
2
3 like features of Micro-Ti being markedly diminished with the fresh EA. Both systems
4 resulted in the formation of nanopores along the machined lines of the Micro-Ti. The
5 average diameter of nanopores on titanium for fresh and aged EA is 28 nm and 30 nm,
6 respectively. The formation of pores instead of tubes can be attributed to: reduced
7 water content, less voltage/time, lack of surface smoothing and the EA performed in
8 a controlled environment.¹² Interestingly for aged EA, the nanopores were
9 superimposed on the underlying micro-groove like architecture, thereby resulting in a
10 dual micro- and nano-scale surface (Figure 1g-i). The micro-scale grooves of the ‘as-
11 received’ machined Ti (Figure 1a,b) served as the template, allowing self-ordering of
12 the nanopores along these lines. Clearly, for the aged system the nanopores can be
13 seen aligned (Figure 1i) in the direction of the machining imprints (micro-scale lines,
14 as seen in Figure 1b). On the contrary, for the fresh EA system, both of these features
15 were diminished, with reduced alignment of the nanopores (Figure 1f) along the
16 micro-machining lines of the Micro-Ti.
17
18
19
20
21
22
23
24
25

26 Interestingly, 1st anodized nanoporous structures have been reported previously,
27 however have not been applied towards specific applications (especially
28 orthopaedic/dental implants).¹³ Conventionally, these 1st anodized anodic films are
29 removed to perform a 2nd EA on a template surface. A few studies have aimed at
30 utilizing the dual micro-nano architecture to display augmented cellular functions, but
31 only using multiple technologies combined with EA.⁹⁻¹¹ The ability to achieve such
32 features via a single-step EA can enable easy and cost-effective clinical translation.
33 Furthermore, more recently we have demonstrated that aligned nanopores can enable
34 selective bioactivity, whereby proliferation and adhesion of osteoblasts and fibroblasts
35 is enhanced, and macrophage functionality is reduced.¹⁴ Additionally, osteoblasts and
36 fibroblasts aligned in the direction of the nanopore arrangement, clearly suggesting
37 strong mechanical stimulation from these nanostructures.¹⁴ It is also noteworthy that a
38 variety of cells are able to respond to mechanical and topographical cues, and hence
39 changing the micro- and nano-dimensions (simply by varying anodization conditions)
40 can further aid in achieving tailored cellular and therapeutic responses.^{2,15}
41
42
43
44
45
46
47
48
49
50
51
52
53
54
55
56
57
58
59
60

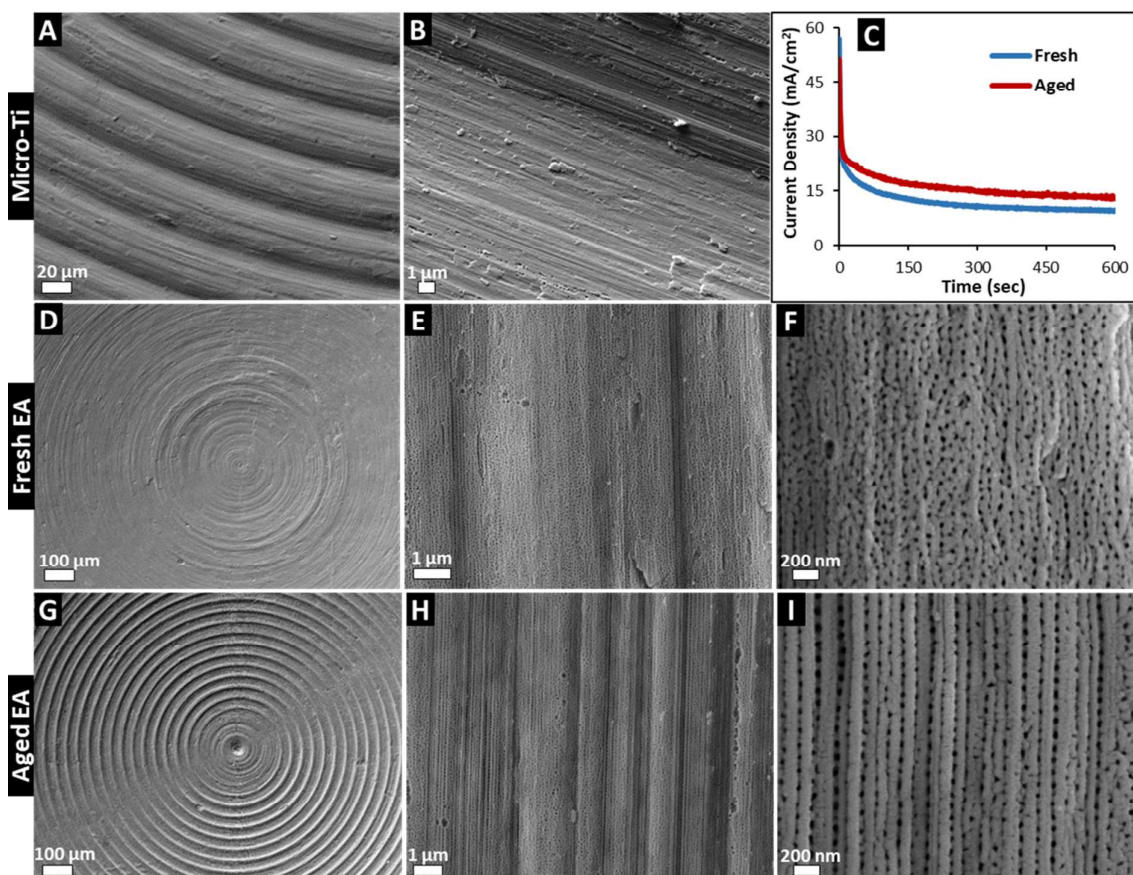


Figure 1. Electrochemical anodization (EA) of micro-machined Ti implants (Micro-Ti). Top-view SEM images: (a-b) bare Micro-Ti, (d-f) Micro-Ti anodized with fresh electrolyte, and (g-i) anodized in aged electrolyte. (c) Current density vs time plots comparing EA using fresh and aged electrolytes. EA performed at 60V 10m.

It is well known that nanotubes/pores grow perpendicular to the surface of the substrate, in the direction of the electric field. If the surface contains inconsistencies in the form of artefacts or impurities, the high concentration electric field at these points may result in very high local current densities, yielding defects in the anodic film.^{7,16} Besides, the electric field intensity is expected to be higher at the topographical minima of the substrate, i.e. minima of the ‘crest and trough’-like architecture. The implant substrate used in this study not only has micro-scale features (crests and troughs), but also has a surface which is entirely decorated with a unidirectional machined lining (Figure 1a-b). The high intensity of the electric field at these points (‘weak spots’) further enhances the oxidation-dissolution rates, which is more prominent for the fresh EA system (‘consumption’).¹⁷ The growth phase is also

1
2
3 characterized by the continuous dissolution and rebuilding of the compact barrier layer
4 (BL) at the pore bottom-electrolyte interface; and for a high electric field
5 concentration (fresh electrolyte); high growth rates can effectively lead to
6 consumption of substrate micro-features.¹⁸⁻¹⁹ This can explain the ‘blunting’ of the
7 micro-features of the machined titanium substrate, yielding an almost flat surface, for
8 the fresh EA system (Figure 1d-f).
9
10
11

12
13 In contrast to other electrolyte ageing approaches where the conductivity increases
14 (due to higher TiF_6^{2-} and water content in the electrolyte); in a moisture-controlled
15 system the conductivity continuously reduces with each EA, which is mainly
16 attributed to the consumption of water.⁷ We have also observed an increase in O_2
17 bubbles at the oxide-electrolyte interface for fresh EA, as compared to a sparse bubble
18 production for the aged EA. We have also shown previously that the increased time
19 required to reach an EA equilibrium stage, as well as the reduced rates of formation
20 and dissolution of the oxide, contribute towards the generation of mechanically stable
21 nanostructures, especially on a complex substrate with many ‘weak spots’.⁷
22
23
24
25
26
27

28 As presented in Figure 1g-i, the aged EA enables generation of a hybrid micro-nano
29 architecture whereby an anodic film with nanopores is superimposed on the micro-
30 patterned Ti implant. Furthermore, as observed in the SEM images (Figure 1f,i), it is
31 clear that the underlying micro-machining enables pore alignment, whereby the
32 pores/tubes aligned in the direction of the grooves on the mechanically polished Ti.
33 However, it is interesting to note that the alignment of pores along the underlining
34 machined surface is better for aged-EA, as compared to fresh-EA. This again can be
35 attributed to increased preservation of these micro-machining lines (serving like a
36 template) in the aged EA (water and fluoride constraints impeding both oxidation and
37 dissolution reaction rates). It is noteworthy that the dimples/template features of the Ti
38 substrate acts as initiation sites for tube/pore growth, and hence can result in specific
39 arrangements.
40
41
42
43
44
45
46
47

48 Presence of active fluoride ions in the electrolyte can significantly influence the EA
49 process.^{1,7} Fluoride accumulation at the nanotube/nanopore bottoms in the form of
50 soluble species (Ti-O-F , Ti-F complexes) also forms an additional F-rich layer
51 between the BL and the substrate.²⁰ In addition, for a fluoride-rich fresh electrolyte,
52 the fluoride attack can be more prominent at the defect sites (in our study: presence of
53 micro-machining lines, and micro-architecture: crest and troughs). In fact, it has been
54
55
56
57
58
59
60

1
2
3 reported that water content in fluoride-containing electrolytes can caused increased
4 expansion [Pilling–Bedworth ratio (PBR)] that can lead to stress and volume
5 difference between anodic layer and substrate.²¹ For an aged system, with reduced
6 water (and fluoride content) reduced expansion rates can be assumed, which in our
7 investigation led to improved preservation of both the micro-machining lines (better
8 nanopore alignment on the micro-templated Ti) and the ‘crest and trough’ like micro-
9 architecture (dual micro-nanoporous).

10
11 To further investigate why the micro-features were poorly or well preserved in
12 specific electrolyte systems, we observed the early time points in the EA, using 60V
13 and 100V for 60sec. The top view SEM images and corresponding current density-
14 time plots are presented in Figure 2. For both 60 and 100V, in the first 15 sec, there is
15 no significant difference between the current density values for fresh and aged
16 systems, however after 15 sec, clearly $J_{\text{aged}} > J_{\text{fresh}}$ (Figure 2e-h). This co-relates to
17 the delayed time to reach equilibrium (established through the barrier oxide layer at
18 the nanopore bases) and thicker barrier layers (for aged EA).⁷ It has also been
19 recognized that the fluoride-rich layer at the metal-oxide interface is attributed to
20 faster inward fluoride ion migration under high electric fields.²²⁻²³ Clearly for a fresh
21 system with an abundance of fluoride ions, rapid fluoride migration to the metal-oxide
22 interface occurs, which is followed by chemical dissolution of these fluoride-rich
23 layers in water, resulting in a tubular morphology (consumption of surface micro-
24 features over time).²⁴ On the contrary, in a fluoride and water deficient aged system,
25 the formation/solubility of this layer is impeded, thereby preserving the underlying
26 substrate features and continuing with the EA-assisted growth of nanotubes/pores. The
27 perpendicular growth of tubes/pores thereby results in surface defects (due to field
28 concentration effects), as shown in Figure 2j,l, for the aged-EA. This finding is similar
29 to the observed cracks/voids on the anodic film on curved surfaces of Ti wire, as
30 reported previously.⁷ However, it is worth noting that over time, these surface
31 imperfections are reduced with continued EA, as shown for 60V-10m EA in the aged-
32 system (Figure 1h-i).

33
34
35
36
37
38
39
40
41
42
43
44
45
46
47
48
49
50
51
52
53
54
55
56
57
58
59
60

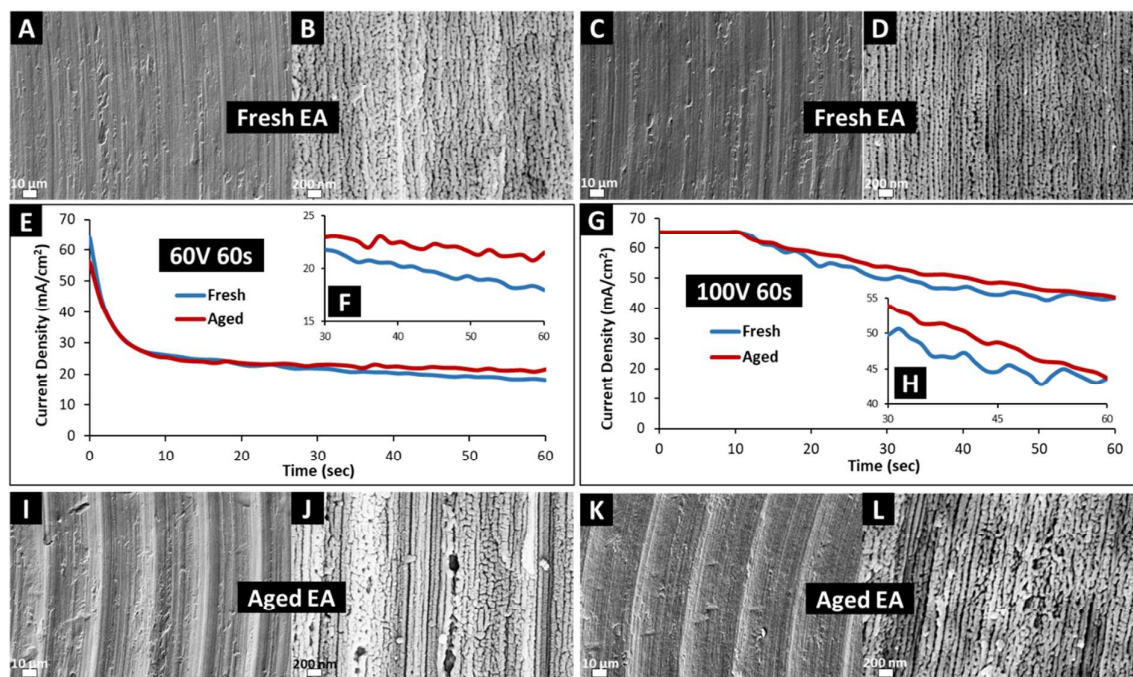
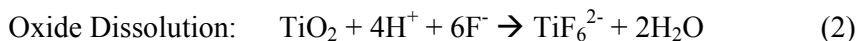
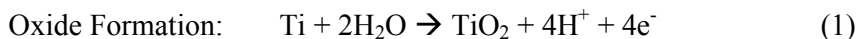


Figure 2. Comparison of electrochemical anodization (EA) of micro-machined Ti in fresh and aged electrolyte systems at 60/100V for 60 sec. Top-view SEM images: (a-b) Fresh EA 60V, (c-d) Fresh EA 100V, (i-j) Aged EA 60V, and (k-l) Aged EA 100V. Current density vs time plots: (e-f) 60V 60sec, and (g-h) 100V 60sec.

To simplify, we have schematically represented the EA procedure (Figure 3) for fresh and aged electrolyte systems to correlate with the SEM images shown in Figure 1-2. It is well established that the electrochemical equilibrium established as per the following chemical reactions tunes the balance between TiO_2 formation and its dissolution, leading to the self-ordering of nanotubes/pores.^{1,10}



Following the Le Chatelier's equilibrium principle, for an aged system, clearly the scarcity of water in the electrolyte reduces the oxide formation rate (1), while the presence of TiF_6^{2-} reduces the oxide dissolution rate (2), both leading to a reduced rate of nanotube/nanopore growth. For fresh EA, representing a rapid formation and dissolution system, an increased build-up of compressive stress at the early EA phase occurs when metal converts to oxide (volume expansion: Pilling-Bedworth ratio or PBR).²⁴⁻²⁵ Over time, this results in the consumption of the micro-features of the Ti, as shown in Figure 3a. On the

1
2
3 contrary, in an aged system, whereby the dissolution is severely impeded, the compressive
4 stress may be ‘frozen’ in the compact oxide layer, as reported elsewhere.²⁴⁻²⁵ Although with
5 numerous parameters influencing the metal-oxide interface, it is difficult to elucidate the
6 exact mechanism behind the varied EA behavior observed for fresh and aged systems, clearly
7 reduced water and fluoride content for aged-EA induces surface defects, increased time to
8 reach equilibrium current value, and reduced etching of grain boundaries, all leading to well
9 preserved underlying substrate features with superimposed anodic nanopore film.²⁶⁻²⁷
10 Furthermore, it is established that EA on a nano-templated substrate (obtained after removal
11 of the anodic film) results in improved ordering, however this approach may completely
12 remove the underlying implant features. Our strategy (single step EA with conditioned
13 electrolyte) may be beneficial for applications such as the ability to preserve the ‘gold
14 standard’ micro-features of dental implant surfaces, which have been shown to improve early
15 bone formation and osseointegration.⁸

16
17
18
19
20
21
22
23
24 In the current study, for EA in a shielded electrochemical setup (avoiding moisture
25 uptake by the hygroscopic electrolyte: throughout ageing using dummy titanium and
26 anodization of target substrate), the pH of the electrolyte increased from 6.65 for fresh
27 electrolyte to almost 7.90 (averaged values) for a 10 hr aged electrolyte. It is interesting that
28 other electrolyte ageing studies report a reduced pH, however, that may be attributed to a
29 continued water absorption over time (which also leads to an increased conductivity).⁶⁻⁷ For
30 our study, this effect can easily be explained by continued consumption of water which leads
31 to reduced titanium hydrolysis (equation 1), lesser H⁺ production and hence a relatively
32 higher pH value.²⁸ Various investigations have also stressed the importance of pH on
33 anodization yield, however, pH at the nanotube/pore tips and the bottoms is controlled by the
34 bulk electrolyte and self-acidification process, respectively.²⁹ Here, the self-acidification at
35 the tube-bottoms is in turn effected by the chemistry of the electrolyte; notably in aged
36 electrolyte this is related to the water and fluoride constraints.³⁰ Briefly, it is established that
37 for a basic electrolyte pH, both the oxide formation (equation 1) and the chemical dissolution
38 (equation 2) rates are reduced.²⁹ Therefore, a decreased rate of electrochemical etching at the
39 tube bottom for aged electrolyte (pH 7.9) as compared to fresh electrolyte (pH 6.65) may also
40 explain the ‘conserving’ of the substrate micro-features.

41
42
43
44
45
46
47
48
49
50
51
52
53
54
55
56
57
58
59
60

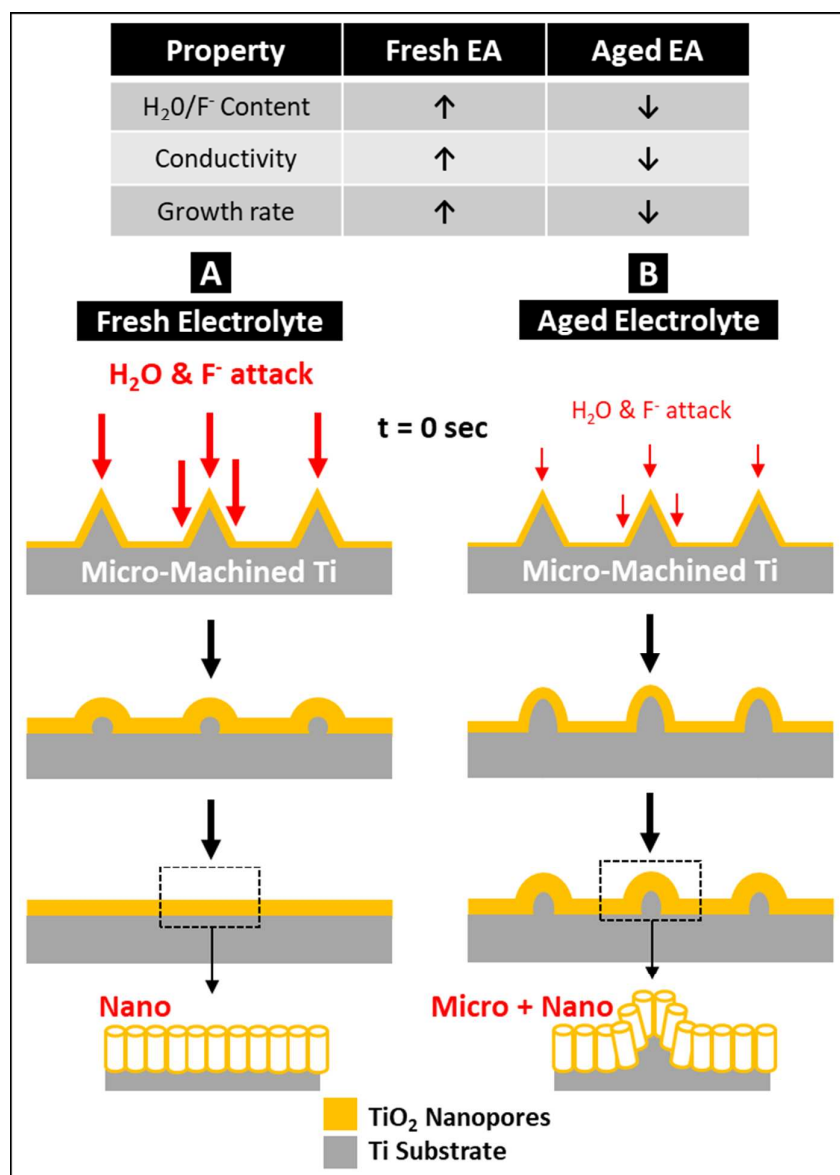


Figure 3. Schematic illustration of the varied electrochemical anodization (EA) reactions based on electrolyte age (fresh/unused and aged) on (a) ‘consuming’ [higher fluoride and water attack] and (b) ‘conserving’ [reduced fluoride and water attack] the underlying micro-roughness of a titanium substrate, towards generation of nanoporous and dual micro-nanoporous topographies, respectively. Table summarizes the difference in water/fluoride content between the fresh and aged electrolytes, as well as the corresponding EA properties.

It is worth noting that for conventional nanotubes, the gap between the individual tubes can make them prone to fracture and hence can be less mechanically robust.²⁷⁻³¹ On the contrary, nanopores are compactly interconnected with the surrounding pores enabling

sharing/distribution of external compression forces.^{27,32} To evaluate the mechanical stability of the as-fabricated dual micro-nano Ti implants, we investigated and compared the elastic modulus and hardness of the nanopores anodized with fresh and aged systems (Table 1). Nanoindentation testing revealed a dependence of the modulus on the displacement depth of the indenter, and clearly for both systems, the modulus increased with depth, which can be attributed to the presence of underlying substrate and densification.^{27,33} However, aged EA yielded nanopores with increased modulus and hardness values as compared to the corresponding depth for fresh EA. These observations are also in agreement with our previous study, whereby we obtained improved stability of anodic films when more time was taken for the current to reach a steady-state value (equilibrium).⁷ Interestingly, the dual micro-rough and nanoporous structures fabricated using aged EA demonstrated increased modulus and hardness values. This is also in accordance with a study by Wang et al., which showed that a laser pre-treated micro-rough surface significantly enhanced the adhesive strength between nanostructure layers and the underlying substrate, mainly due to the expanded interfacial area.¹⁰

Displacement (nm)	Elastic Modulus (GPa)		Hardness (GPa)	
	Aged	Fresh	Aged	Fresh
50	44.34±15.1	44.90±9.5	2.32±1.5	1.73±0.5
100	55.45±10.3	46.09±2.4	2.18±0.4	1.36±0.1
150	59.84±11.1	50.33±3.3	2.45±0.5	1.33±0.1
200	69.21±16.7*	57.38±3.8* [#]	2.63±0.7	1.36±0.1
250	73.05±12.1*	58.85±7.1* [#]	2.83±0.6	1.43±0.2
300	73.91±10.6*	61.32±7.4* [#]	2.93±0.5	1.48±0.3

Table 1 Comparing the mechanical properties of the nanoporous surface on the micro-machined titanium implants, anodized (60V 10m) using aged and fresh electrolytes, using Nanoindentation testing. Measurements represent a mean value of at least 3 indentation measurements performed on each sample (total 3 samples) [*: p<0.05 compared with values from 50 nm within the same group, [#]: p<0.05 compared with values from 100 nm within the same group].

1
2
3 While the results of this study demonstrated the ability to decide between ‘consumption
4 or conservation’ of substrate micro-features, towards fabrication of dual micro-and
5 nanoporous titanium for implantable applications, there are a few challenges with respect to
6 determining the precise mechanism involved (with respect to role of electrolyte ageing, based
7 on current established models).³⁴⁻³⁵ These briefly include: (a) surface micro-features (crest
8 and trough) and micro-machining lines cause extreme irregularity with respect to the electric
9 field distribution; (b) the monotonic current density decrease with time causes issues with
10 estimating J_{\max} or J_{\min} (and corresponding BL), especially for a short duration (and less
11 voltage) of anodization; and (c) the complex chemical balance of fluoride and water
12 constraints with excess Ti ions (aged electrolyte). Apolinário *et al.* have described these
13 factors in detail for a more conventional Ti EA with fresh electrolytes, and longer EA times
14 (with higher voltages).³⁴⁻³⁵ We believe the abovementioned challenges must be met to
15 correctly estimate and match the established EA models used to describe the growth kinetics
16 dependent on various EA parameters (more importantly on Ti substrate roughness and
17 conditioned electrolyte: both of which were at play in this study).
18
19
20
21
22
23
24
25
26

27
28 The results of this study provide evidence that for electrochemical anodization of micro-
29 rough titanium implant, electrolyte ageing can enable preservation of the underlying implant
30 micro-features (especially relevant to ensure initial implant interlocking/stability), thereby
31 yielding a dual micro-nano surface. The findings compared the short-time anodization
32 between fresh (unused) and aged electrolytes, to elucidate how electrolyte conditioning
33 contributes towards the ‘consumption or conservation’ of the underlying micro-roughness.
34 Bypassing the complicated multi-step procedures, this cost-effective single-step anodization
35 technique with aged electrolyte yielded mechanically-stable aligned nanopores superimposed
36 on the micro-scale features of the implant, enabling multi-functionality (micro: initial
37 stability, and nano: bioactivity and drug release) and thereby ensuring easy translation into
38 current implant market.
39
40
41
42
43
44
45
46
47

48 **Conflict of interest**

49 There are no conflicts to declare.
50
51
52
53
54
55
56
57
58
59
60

Acknowledgements

KG is supported by the National Health and Medical Research Council (NHMRC) Early Career Fellowship (ECF), Peter Doherty-Australian Biomedical Fellowship (APP1140699). Authors would like to thank the support from Central Analytical Research Facility (CARF) at Queensland University of Technology (QUT), Brisbane, Australia.

References

1. Roy, P.; Berger, S.; Schmuki, P. TiO₂ nanotubes: synthesis and applications. *Angew. Chem. Int. Ed.* **2011**, *50*, 2904 – 2939. <https://doi.org/10.1002/anie.201001374>
2. Gulati, K.; Maher, S.; Findlay, D. M.; Losic, D. Titania Nanotubes for Orchestrating Osteogenesis at the Bone-Implant Interface. *Nanomed. (Lond.)* **2016**, *11*, 1847–1864. <https://doi.org/10.2217/nnm-2016-0169>
3. Lee, K.; Kim, J.; Kim, H.; Lee, Y.; Tak, Y.; Kim, D.; Schmuki, P. Effect of electrolyte conductivity on the formation of a nanotubular TiO₂ photoanode for a dye-sensitized solar cell. *J. Korean Phys. Soc.* **2009**, *54*, 1027–1031. DOI: 10.3938/jkps.54.1027
4. Zhu, W.; Liu, X.; Liu, H.; Tong, D.; Yang, J.; Peng, J. An efficient approach to control the morphology and the adhesion properties of anodized TiO₂ nanotube arrays for improved photoconversion efficiency. *Electrochim. Acta* **2011**, *56*, 2618–2626. <https://doi.org/10.1016/j.electacta.2010.11.012>
5. Jarosz, M.; Pawlik, A.; Kapusta-Kołodziej, J.; Jaskuła, M.; Sulka, G. D. Effect of the previous usage of electrolyte on growth of anodic titanium dioxide (ATO) in a glycerol-based electrolyte. *Electrochim. Acta* **2014**, *136*, 412–421. <https://doi.org/10.1016/j.electacta.2014.05.077>
6. Costa, J. D.; Quitério, P.; Apolinário, A.; Sousa, C. T.; Azevedo, J.; Ventura, J.; Andrade, L.; Mendes, A.; Araújo, J. P.. The effect of electrolyte re-utilization in the growth rate and morphology of TiO₂ nanotubes. *Mater. Lett.* **2016**, *171*, 224–227. <https://doi.org/10.1016/j.matlet.2016.02.085>

- 1
2
3 7. Gulati, K.; Santos, A.; Findlay, D.; Losic, D. Optimizing anodization conditions for
4 fabricating well-adherent and robust titania nanotubes on curved surfaces. *J. Phys. Chem.*
5 *C* **2015**, *119*, 16033–16045. DOI: 10.1021/acs.jpcc.5b03383
6
7
- 8 8. Gulati, K.; Ivanovski, S. Dental implants modified with drug releasing titania nanotubes:
9 therapeutic potential and developmental challenges. *Expert Opin. Drug Deliv.* **2017**, *14*,
10 1009-1024. <https://doi.org/10.1080/17425247.2017.1266332>
11
- 12 9. Peng, W.; Qiao, Z.; Zhang, Q.; Cao, X.; Chen, X.; Dong, H.; Liao, J.; Ning, C.
13 Micropatterned TiO₂ nanotubes: fabrication, characterization and in vitro protein/cell
14 responses. *J. Mater. Chem. B* **2013**, *1*, 3506–3512. DOI:10.1039/C3TB20373E
15
- 16 10. Wang, D.; Hu, T.; Hu, L.; Yu, B.; Xia, Y.; Zhou, F.; Liu, W. Microstructured arrays of
17 TiO₂ nanotubes for improved photo-electrocatalysis and mechanical stability. *Adv. Funct.*
18 *Mater.* **2009**, *19*, 1930-1938. <https://doi.org/10.1002/adfm.200801703>
19
- 20 11. Gulati, K.; Prideaux, M.; Kogawa, M.; Lima-Marques, L.; Atkins, G. J.; Findlay, D. M.;
21 Losic, D. Anodized 3D printed titanium implants with dual micro- and nano-scale
22 topography promotes interaction with human osteoblasts and osteocyte-like cells. *J.*
23 *Tissue Eng. Regen. Med.* **2017**, *11*, 3313–3325. <https://doi.org/10.1002/term.2239>
24
- 25 12. Regonini, D.; Bowen, C. R.; Jaroenworarluck, A.; Stevens, R. A review of growth
26 mechanism, structure and crystallinity of anodized TiO₂ nanotubes. *Mater. Sci. Eng. R*
27 **2013**, *74*, 377–406. <https://doi.org/10.1016/j.mser.2013.10.001>
28
- 29 13. Wang, D.; Yu, B.; Wang, C.; Zhou, F.; Liu, W. A novel protocol toward perfect
30 alignment of anodized TiO₂ nanotubes. *Adv. Mater.* **2009**, *21*, 1964-1967.
31 <https://doi.org/10.1002/adma.200801996>
32
- 33 14. Gulati, K.; Moon, H.; Li T.; Kumar, P. T. S.; Ivanovski, S. Titania Nanopores with Dual
34 Micro-/Nano-Topography for Selective Cellular Bioactivity. *Mater. Sci. Eng. C* **2018**, *91*,
35 624-630. <https://doi.org/10.1016/j.msec.2018.05.075>
36
- 37 15. Gulati, K.; Hamlet, S. M.; Ivanovski, S. Tailoring the Immuno-Responsiveness of
38 Anodized Nano-Engineered Titanium Implants. *J. Mater. Chem. B* **2018**, *6*, 2677-2689.
39 DOI: 10.1039/C8TB00450A
40
- 41 16. Fan, M.; La Mantia, F. Effect of surface topography on the anodization of titanium.
42 *Electrochem. Commun.* **2013**, *37*, 91–95. <https://doi.org/10.1016/j.elecom.2013.10.012>
43
- 44 17. Proost, J.; Vanhumbecq, J. F.; Van Overmeere, Q. Instability of anodically formed TiO₂
45 layers (Revisited). *Electrochim. Acta* **2009**, *55*, 350–357.
46 <https://doi.org/10.1016/j.electacta.2008.12.008>
47
48
49
50
51
52
53
54
55
56
57
58
59
60

- 1
2
3 18. Su, Z.; Zhou, W. Formation, microstructures and crystallization of anodic titanium oxide
4 tubular arrays. *J. Mater. Chem.* **2009**, *19*, 2301-2309. DOI: 10.1039/B820504C
5
6 19. Sulka, G. D.; Kapusta-Kołodziej, J.; Brzózka, A.; Jaskuła, M. Fabrication of nanoporous
7 TiO₂ by electrochemical anodization. *Electrochim. Acta* **2010**, *55*, 4359-4367.
8 <https://doi.org/10.1016/j.electacta.2009.12.053>
9
10 20. Macak, J. M.; Tsuchiya, H.; Ghicov, A.; Yasuda, K.; Hahn, R.; Bauer, S.; Schmuki, P.
11 TiO₂ nanotubes: self-organized electrochemical formation, properties and applications.
12 *Curr. Opin. Solid State Mater. Sci.* **2007**, *11*, 3-18.
13 <https://doi.org/10.1016/j.cossms.2007.08.004>
14
15 21. Albu, S. P.; Schmuki, P. Influence of anodization parameters on the expansion factor of
16 TiO₂ nanotubes. *Electrochim. Acta* **2013**, *91*, 90-95.
17 <https://doi.org/10.1016/j.electacta.2012.12.094>
18
19 22. Kowalskia, D.; Mallet, J.; Thomas, S.; Rysz, J.; Bercu, B.; Michel, J.; Molinari, M. Self-
20 organization of TiO₂ nanotubes in mono-, di- and tri-ethylene glycol electrolytes.
21 *Electrochim. Acta* **2016**, *204*, 287-293. <https://doi.org/10.1016/j.electacta.2016.02.213>
22
23 23. Habazaki, H.; Fushimi, K.; Shimizu, K.; Skeldon, P.; Thompson G. E. Fast migration of
24 fluoride ions in growing anodic titanium oxide. *Electrochem. Commun.* **2007**, *9*, 1222-
25 1227. <https://doi.org/10.1016/j.elecom.2006.12.023>
26
27 24. Zhou, X.; Nguyen, N. T.; Özkan, S.; Schmuki, P. Anodic TiO₂ nanotube layers: why does
28 self-organized growth occur-a mini review. *Electrochem. Commun.* **2014**, *46*, 157-162.
29 <https://doi.org/10.1016/j.elecom.2014.06.021>
30
31 25. Vanhumbecq, J. F.; Proost, J. On the contribution of electrostriction to charge-induced
32 stresses in anodic oxide films. *Electrochim. Acta* **2008**, *53*, 6165-6172.
33 <https://doi.org/10.1016/j.electacta.2007.11.028>
34
35 26. Wei, W.; Berger, S.; Hauser, C.; Meyer, K.; Yang, M.; Schmuki, P. Transition of TiO₂
36 nanotubes to nanopores for electrolytes with very low water contents. *Electrochem.*
37 *Commun.* **2010**, *12*, 1184-1186. <https://doi.org/10.1016/j.elecom.2010.06.014>
38
39 27. Li, T.; Gulati, K.; Wang, N.; Zhang, Z.; Ivanovski S. Understanding and Augmenting the
40 Stability of Therapeutic Nanotubes on Anodized Titanium Implants. *Mater. Sci. Eng. C*
41 **2018**, *88*, 182-195. <https://doi.org/10.1016/j.msec.2018.03.007>
42
43 28. Macak, J. M., Schmuki, P. Anodic growth of self-organized anodic TiO₂ nanotubes in
44 viscous electrolytes. *Electrochim. Acta* **2006**, *52*, 1258-1264.
45 <https://doi.org/10.1016/j.electacta.2006.07.021>
46
47
48
49
50
51
52
53
54
55
56
57
58
59
60

- 1
2
3 29. Feng, X.; Macak, J. M.; Schmuki, P. Robust Self-Organization of Oxide Nanotubes over
4 a Wide pH Range. *Chem. Mater.* **2007**, *19*, 1534-1536. DOI: 10.1021/cm063042g
5
6 30. Raja, K. S.; Gandhi, T.; Misra, M. Effect of water content of ethylene glycol as
7 electrolyte for synthesis of ordered titania nanotubes. *Electrochem. Commun.* **2007**, *9*,
8 1069–1076. <https://doi.org/10.1016/j.elecom.2006.12.024>
9
10 31. Crawford, G.; Chawla, N.; Das, K.; Bose, S.; Bandyopadhyay, A. Microstructure and
11 Deformation Behavior of Biocompatible TiO₂ Nanotubes on Titanium Substrate. *Acta*
12 *Biomater.* **2007**, *3*, 359-367. <https://doi.org/10.1016/j.actbio.2006.08.004>
13
14 32. Hirakata, H.; Ito, K.; Yonezu, A.; Tsuchiya, H.; Fujimoto, S.; Minoshima, K. Strength of
15 self-organized TiO₂ nanotube arrays. *Acta Mater.* **2010**, *58*, 4956-4967.
16 <https://doi.org/10.1016/j.actamat.2010.05.029>
17
18 33. Xu, Y. N.; Liu, M. N.; Wang, M. C.; Oloyede, A.; Bell, J. M.; Yan, C. Nanoindentation
19 study of the mechanical behavior of TiO₂ nanotube arrays. *J. Appl. Phys.* **2015**, *118*,
20 145301. <https://doi.org/10.1063/1.4932213>
21
22 34. Apolinário, A.; Sousa, C. T.; Ventura, J.; Costa, J. D.; Leitão, D. C.; Moreira, J. M.;
23 Sousa, J. B.; Andrade, L.; Mendes, A. M.; Araújo, J. P. The role of the Ti surface
24 roughness in the self-ordering of TiO₂ nanotubes: a detailed study of the growth
25 mechanism. *J. Mater. Chem. A* **2014**, *2*, 9067-9078. DOI: 10.1039/C4TA00871E
26
27 35. Apolinario, A.; Quiterio, P.; Sousa, C. T.; Ventura, J.; Sousa, J. B.; Andrade, L.; Mendes,
28 A. M.; Araujo, J. P. Modeling the Growth Kinetics of Anodic TiO₂ Nanotubes. *J. Phys.*
29 *Chem. Lett.* **2015**, *6*, 845–851. DOI: 10.1021/jz502380b
30
31
32
33
34
35
36
37
38
39
40
41
42
43
44
45
46
47
48
49
50
51
52
53
54
55
56
57
58
59
60

For Table of Contents Use Only

Consume or Conserve: Micro-Roughness of Titanium Implants towards Fabrication of Dual Micro-Nano Topography

Karan Gulati^{a,b,c}, Tao Li^{b,d}, and Sašo Ivanovski^{a,b,c}

^a The University of Queensland, School of Dentistry, Herston, QLD 4006, Australia

^b School of Dentistry and Oral Health, Griffith University, Gold Coast, QLD, Australia

^c Menzies Health Institute Queensland (MHIQ), Griffith University, Gold Coast, QLD, Australia

^d Department of Prosthodontics, School of Stomatology, Capital Medical University, Beijing, People's Republic of China

